

The 3Fe containing ferredoxin from *Desulfovibrio gigas*: an NMR characterization of the oxidised and intermediate states

Anjos L. Macedo ^{a,*}, Pedro Rodrigues ^a, Brian J. Goodfellow ^b

^a Departamento de Química, C.Q.F.B., Faculdade de Ciências e Tecnologia,
Universidade Nova de Lisboa, 2825 Monte de Caparica, Portugal

^b Departamento de Química, Universidade de Aveiro, 3810 Aveiro, Portugal

Received 11 September 1998; accepted 6 April 1999

Contents

Abstract	871
1. Introduction	872
2. NMR characterization of FdII _{ox}	873
2.1 Coupling between the iron atoms in the [3Fe–4S] cluster	874
2.2 The solution structure of FdII _{ox}	876
3. Characterization of the intermediate state, FdII _{int}	878
4. Conclusions	879
Acknowledgements	879
References	880

Abstract

Ferredoxin II (FdII), isolated from *Desulfovibrio gigas*, is a small electron transfer protein that contains one [3Fe–4S] cluster per monomer (6 kDa). The characterization of the oxidized and intermediate forms of FdII was carried out by NMR spectroscopy, in conjunction with other spectroscopic techniques, such as EPR, UV–vis and Mössbauer spectroscopy, in order to fully understand the redox and electronic properties of the protein. The native oxidized state of FdII has been studied from the point of view of the spin coupling between the iron atoms, via the ¹H-NMR temperature dependence of the β-CH₂ proton resonances of the cysteinyl cluster ligands (Cys8, Cys14 and Cys50). The assignment of the 2D-NOESY spectrum has also been carried out: distances have been obtained for the

* Corresponding author. Tel.: +351-1-2954464 (ext.0965); fax: +351-1-2948550.

E-mail address: alm@dq.fct.unl.pt (A.L. Macedo)

diamagnetic region and 1D-NOE experiments were performed in order to detect NOEs for protons in the vicinity of the cluster, allowing the determination of the protein structure in solution. An intermediate state, FdII_{int} , detected by NMR spectroscopy, was attributed to the opening of the S–S bridge between Cys18 and Cys42, in the potential range of cluster reduction. This state has been characterized by several spectroscopic techniques, showing that the protein can transfer three electrons in one redox step, that involves the $[\text{3Fe–4S}]$ cluster and the disulfide bridge. The temperature behavior of the hyperfine shifts, when compared with FdII_{ox} , lead to the conclusion that the spin coupling of the cluster changes upon reduction of the S–S bond. 2D-NOESY spectra of the diamagnetic region were also collected for FdII_{int} , and compared with the native state, in order to clarify the structural changes occurring in the protein on cleavage of the S–S bridge. © 1999 Elsevier Science S.A. All rights reserved.

Keywords: ^1H -NMR; Paramagnetic system; Electronic structure; Solution structure; Ferredoxin; $[\text{3Fe–4S}]$

1. Introduction

Ferredoxins (Fd) are small electron transfer proteins with iron and sulfide at the active site. The iron atoms are high spin Fe^{2+} or Fe^{3+} , bound tetrahedrally by sulfur atoms which can be bridging or terminal in nature (although other atoms, such as O or N, may be involved) [1]. Four distinct types of ferredoxins are found in sulfate reducing bacteria (SRB): 3Fe Fds containing one $[\text{3Fe–4S}]$ cluster, 4Fe Fds containing one $[\text{4Fe–4S}]$ cluster, 7Fe Fds containing a $[\text{3Fe–4S}]$ and a $[\text{4Fe–4S}]$ cluster, and 8Fe Fds containing two $[\text{4Fe–4S}]$ clusters [2–4]. The $[\text{3Fe–4S}]$ cluster with its intriguing structure, a cubane lacking a corner iron atom, and the capability to incorporate an additional iron or other transition metal atoms [5–7] demonstrates the structural versatility of iron–sulfur clusters.

The $[\text{3Fe–4S}]$ cluster can be stabilized in solution in two oxidation states: $[\text{3Fe–4S}]^{1+}$ and $[\text{3Fe–4S}]^0$. In the oxidized state, $[\text{3Fe–4S}]^{1+}$, the three high-spin ferric atoms ($S = 5/2$) are antiferromagnetically coupled, forming a electronic ground state with a spin system of $1/2$ [8,9]. The one electron reduced state, $[\text{3Fe–4S}]^0$, contains a mixed valence pair, $2 \times \text{Fe}^{+2.5}$, with $S = 9/2$, and one Fe^{3+} , $S = 5/2$. The system is characterized by a global $S = 2$ spin state, arising from antiferromagnetic coupling between the two spin systems [10–12].

In the case of iron–sulfur proteins, NMR has been invaluable for the elucidation of solution state structures and also in the investigation of the electronic structure of the clusters [13]. The presence of a paramagnetic cluster (or a diamagnetic cluster, which, at room temperature, due to a fractional population of paramagnetic excited states, can be paramagnetic) causes efficient nuclear relaxation, resulting in broadening of resonances, and hyperfine chemical shifts which place the signals well outside the normal diamagnetic envelope (0–10ppm for ^1H) [14,15]. Paramagnetic interactions are most severe for protons close to the metal center, namely the $\beta\text{-CH}_2$ protons of the cysteinyl cluster ligands that feel the unpaired electron spin via delocalisation through chemical bonds (contact effect) and via a ‘through space’ pseudocontact effect.

Desulfovibrio gigas (*D. gigas*) is a SRB from which the 3Fe containing ferredoxin, FdII, is purified. Ferredoxin II is a small protein of 58 amino acids with one [3Fe–4S] cluster per monomer [16,17]. In the native state the protein is a tetramer, that is easily converted to dimer after a redox cycle. The polypeptide chain contains six cysteinyl residues and only one aromatic residue, a phenylalanine (Phe22). The cluster is bound by Cys8, Cys14 and Cys50; Cys11 is available to bind the fourth iron forming a [4Fe–4S] cluster. The two remaining cysteines, Cys18 and Cys42, form a disulfide bridge in the native state, FdII_{ox}, as seen by X-ray crystallography [18] and as detected by NMR spectroscopy [19]. Fig. 1 displays the X-ray structure of FdII, where the features described above are illustrated.

2. NMR characterization of FdII_{ox}

The *D. gigas* FdII in its native form, FdII_{ox}, contains a [3Fe–4S] cluster in the 1+ oxidation state ($S = 1/2$), and its ¹H-NMR spectrum presents four broad resonances in the low-field region, 15–30 ppm (Fig. 2A). These resonances have characteristic features, due to the paramagnetic center, such as short longitudinal relaxation times (T_1), large linewidths and chemical shifts outside the diamagnetic region. The closest protons to the iron atoms are the β -CH₂ protons of the cysteinyl binding ligands. In order to specifically assign these low-field resonances, NMR experiments such as 1D-NOE (tailored to detect fast relaxing signals) and 2D-NOESY (with short mixing times, of the order of the T_1 s of the resonances



Fig. 1. X-ray structure of *D. gigas* FdII [18]. The [3Fe–4S] cluster is bound to the polypeptide chain by Cys8, Cys14 and Cys50. Cys11 is tilted away from the cluster. The aromatic ring of Phe22 is shown as well as the S–S bridge between Cys18 and Cys42.

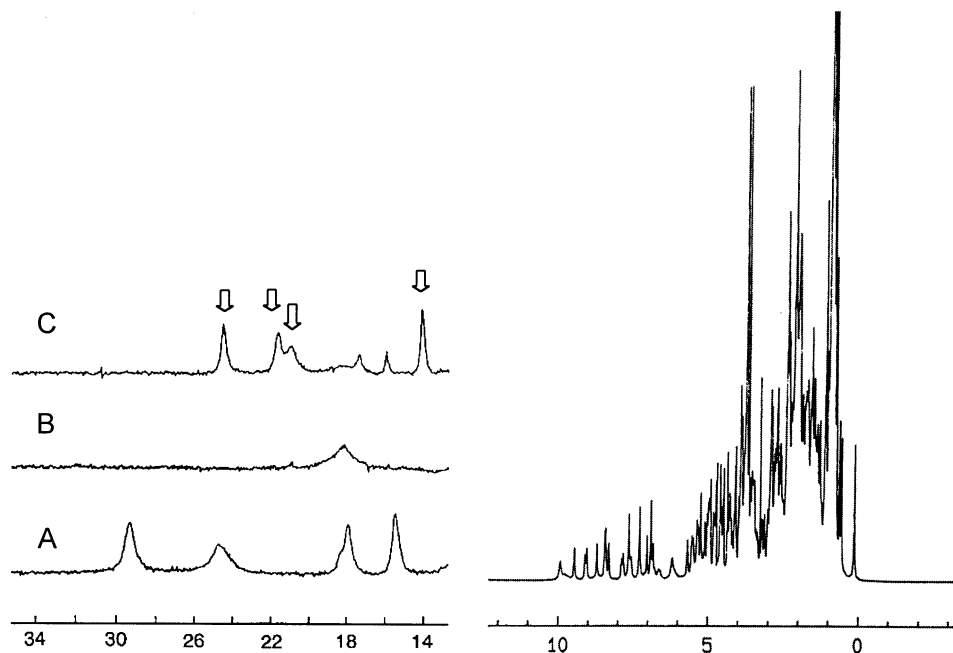


Fig. 2. ¹H-NMR spectra of *D. gigas* FdII. (A) Full spectrum of the oxidized (native) form, with low-field expanded region. Low-field region of the reduced, FdII_{red} (B) and intermediate, FdII_{int} (C) states. The arrows indicate the four resonances that characterize the intermediate state (the sample is in equilibrium with FdII_{red} and a small amount of interconverted [4Fe–4S] protein) (adapted from [19,20]).

involved), were performed [20,21]. The assignment of the C14 β-CH₂ protons to resonances at 15.3 and 8.6 ppm, were made via 1D- and 2D-NOEs detected between these signals and the F22 aromatic resonances (Fig. 3C, D). From the X-ray coordinates [18], of the binding cysteines, only the β-CH₂ protons of Cys14 are less than 5 Å from the aromatic protons of Phe22. Table 1 summarizes the specific assignment and the ¹H-NMR characteristics of the β-CH₂ and α-CH proton resonances of the three cysteinyl cluster ligands.

In the reduced state, FdII_{red}, the low-field region of the ¹H-NMR spectrum, between 15 and 30 ppm, displays only one resonance at 18 ppm (Fig. 2B). Other resonances can be seen at very low-field (ca. 200 ppm), with linewidths of about 2000 Hz, along with resonances in the high-field region at –12 ppm and at –80 ppm [19,22], that are the result of the increasing of the cluster paramagnetism (*S* = 2) in the 0 (reduced) oxidation state.

2.1. Coupling between the iron atoms in the [3Fe–4S] cluster

The chemical shift temperature dependence of the β-CH₂ resonances of Cys8, Cys14 and Cys50, was used to study the electronic properties of the oxidized cluster [20]. Based on the proposed coupling model for the cluster iron atoms [23,24],

described by the Hamiltonian $H = J_{12}\mathbf{S}_1 \cdot \mathbf{S}_2 + J_{13}\mathbf{S}_1 \cdot \mathbf{S}_3 + J_{23}\mathbf{S}_2 \cdot \mathbf{S}_3$, and the contact shift temperature dependence equation [25,26], the NMR data allowed the determination of the iron–iron spin coupling constants. The β -CH₂ proton resonances of Cys50 were found to have Curie temperature behavior, while the protons of Cys8 and Cys14, had anti-Curie behavior (Fig. 4). This was explained assuming different exchange coupling interactions between the three iron atoms in the cluster, with $J_{13} = J_{23} = J$ and $J_{12} = J + \Delta J$ ($\Delta J > 0$). Values of J ca. 300 cm⁻¹ and $\Delta J/J$ ca. 0.02 were used to fit the experimental data and Fe3, in the model, was assigned to the iron in the cluster bound to Cys50. Similar J values were reported for both [3Fe–4S] clusters of the 7Fe Fds isolated from *Bacillus schlegelii* (*B. schlegelii*) [27] and *Rhodospseudomonas palustris* (*R. palustris*) [28]. The set of determined J values were: $J_{12} = 320$, $J_{23} = 280$, $J_{13} = 290$ cm⁻¹ and $J_{12} = 285$, $J_{13} = 300$, $J_{23} = 320$ cm⁻¹ for *B. schlegelii* Fd, and *R. palustris* Fd, respectively. Comparing these values with those found for *D. gigas* FdII, it was concluded that the magnetic interaction within the [3Fe–4S] cluster is less symmetric for 7Fe Fds. This is in agreement with the fact, that in *B. schlegelii* and *R. palustris* ferredoxins, an extra resonance from the β -CH proton of Cys14 seen for *D. gigas* FdII, is not present in the downfield region of the ¹H-NMR spectrum of 7Fe Fds.

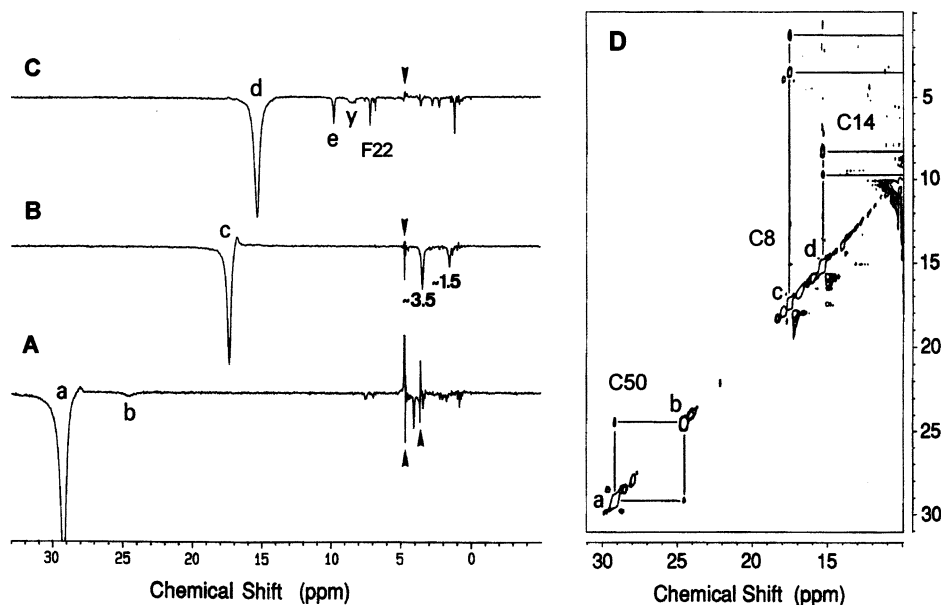


Fig. 3. 1D-NOE spectra of *D. gigas* FdII, after irradiation of the resonances at 29.3 ppm (A), 16.8 ppm (B) and 15.3 ppm (C). (D) The low-field region in the f2 dimension of the 2D-NOESY spectrum (2 ms mixing time). Adapted from Ref. [21].

Table 1

Characteristic features and specific assignment of the proton resonances of the cysteinyl 3Fe cluster ligands in *D. gigas* FdII_{ox} and FdII_{int}[19,20,31]^a

	FdII _{ox}				FdII _{int}			
	δ (ppm)	Proton	T_1 (ms)	$\langle \delta_{\text{cont}} \rangle$ (ppm)	δ (ppm)	Proton	T_1 (ms)	$\langle \delta_{\text{cont}} \rangle$ (ppm)
Cys 8	16.8	β -CH ₂	4.0	7.1	20.8	β -CH ₂	3.2	12.0
	3.0	β' -CH ₂	nd		8.7	β' -CH ₂	nd	
	1.43	α -CH	nd		1.4	α -CH	nd	
Cys 14	15.3	β -CH ₂	7.0	9.2	13.7	β -CH ₂	5.8	8.0
	8.6	β' -CH ₂	nd		7.8	β' -CH ₂	nd	
	9.7	α -CH	nd		9.8	α -CH	16.4	
Cys 50	29.3	β -CH ₂	4.3	24.1	24.1	β -CH ₂	3.6	19.5
	24.4	β' -CH ₂	3.1		20.5	β' -CH ₂	–	
	4.1	α -CH	nd		na	α -CH	–	

^a Data obtained at $T = 300$ K, and 400 MHz. nd: not determined. na: not assigned. $\langle \delta_{\text{cont}} \rangle$: average contact chemical shift for the β -CH₂ cysteinyl protons. The contact chemical shifts were obtained after subtracting 2.8 ppm.

2.2. The solution structure of FdII_{ox}

The determination of the structure of *D. gigas* FdII (in both oxidized and reduced states) in solution, besides the interest in a comparison with the X-ray structure, will allow information to be obtained about the structural modifications occurring in the protein after reduction of the S–S bridge between Cys18 and Cys42, and eventually may explain the cluster behavior in terms of coupling between the iron spins (see Section 3). Questions raised about the oligomerization of this ferredoxin in solution may also be answered by detecting intermonomer NOE effects.

By using standard 2D-NMR experiments (TOCSY and NOESY with mixing times optimized for the detection of diamagnetic spin systems) in combination with 1D-NOE experiments (tailored to detect fast relaxing signals and to correlate resonances in both the paramagnetic and diamagnetic regions) it was possible to assign 51 of the 58 spin systems of *D. gigas* FdII_{ox}. The NMR solution structure was determined using data from 1D-NOE and 2D-NOESY spectra, as distance constraints, in torsion angle dynamics calculations [29]. Information about the spin systems most affected by the cluster paramagnetism was obtained from the X-ray structure. These calculations produced a family of 15 low target function structures (Fig. 5) with a backbone R.M.S.D. value of 0.77 Å. The global fold of the protein in solution is very similar to the solid state; the differences observed, especially those near the [3Fe–4S] cluster, can be attributed to the lack of constraints due to paramagnetic bleaching. A refinement of the structure is underway, using T_1 data obtained from IR-TOCSY (inversion recovery-TOCSY) experiments, collected at different delays [30].

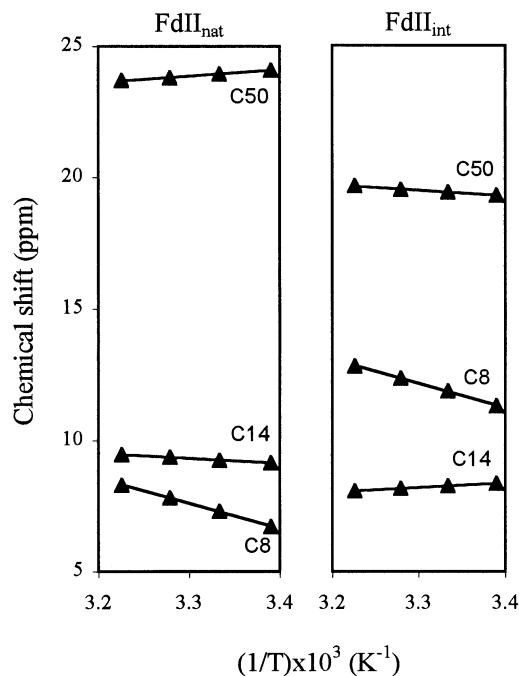


Fig. 4. Temperature dependence of the mean contact shift of the β -CH₂ resonances of the three cysteinyl cluster ligands (Cys8, 14 and 50), for the oxidized (FdII_{nat}) and intermediate states (FdII_{int}) of *D. gigas* FdII [31].

No NOEs which could be directly attributed as intermonomer were seen in the 2D-NOESY spectrum, although some unassigned cross peaks are present which could be possible intermonomer candidates. However, if the dimer is symmetric in solution the inter- and intramonomer interactions will be difficult to distinguish

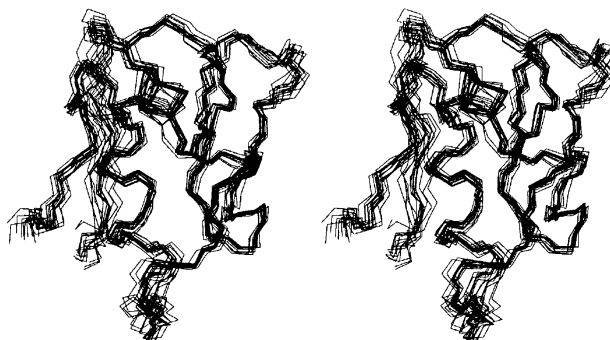


Fig. 5. Stereo view of the superposition of the backbone atoms of the NMR family (15 structures) obtained for the solution structure of *D. gigas* FdII (adapted from Ref. [29]).

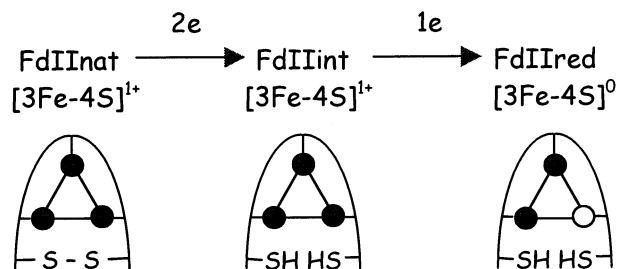


Fig. 6. Schematic representation of the behavior of *D. gigas* FdII at redox potentials of the cluster reduction (−130 mV).

apart. The sharp lines seen in the 1D spectrum suggest that a dimer could be present (12 kDa) in solution and that a tetramer is unlikely.

3. Characterization of the intermediate state, FdII_{int}

¹H-NMR spectroscopy is a sensitive tool for the detection of structural alterations in proteins. A redox study of *D. gigas* FdII identified a stable intermediate state, FdII_{int}, with characteristic hyperfine shifted signals at 24, 21.5, 21 and 14 ppm (Fig. 2C) [19]. This intermediate state appears at redox potentials where the cluster [3Fe-4S]¹⁺ is reduced to the [3Fe-4S]⁰ state (ca. −100 mV) and its characterization by Mössbauer and EPR techniques indicated that the 3Fe cluster remains in the oxidized state. UV-vis redox titrations with methyl viologen indicated that three electrons were required to fully reduce the protein and, as only one electron is needed to reduce the cluster to the [3Fe-4S]⁰ state, the two remaining electrons are used to reduce the disulphide bridge present (in the native state) between Cys18 and Cys42. The intermediate state was therefore postulated to be the protein with the cluster oxidised and the S-S bridge broken (Fig. 6). The differences in chemical shifts found for the lowfield region of the ¹H-NMR spectrum, and Mössbauer spectral changes, on going from FdII_{ox} to FdII_{int} were ascribed to conformational changes resulting from the breaking/formation of this disulfide bridge [19].

The hyperfine shifted ¹H-NMR resonances that characterize FdII_{int} were specifically assigned to the β-CH₂ protons of the cysteinyl cluster ligands, Cys8, Cys14 and Cys50, based on the data obtained from 1D-NOE and 2D-NOESY experiments, and by comparison with FdII_{ox} [31].

The study of the temperature behavior of these resonances showed that one pair of β-CH₂ protons has Curie dependence while the other two have anti-Curie (Fig. 4). A comparison with the same proton resonances in FdII_{ox} showed that the β-CH₂ pair with Curie dependence, belonging to Cys50, is assigned to Cys14 in FdII_{int}. Thus the Fe spin coupling in the cluster appears to be changed by the opening of the disulfide bridge. The model proposed for FdII_{ox} (see Section 2.1.), where a small Δ*J*, i.e. small differences in the iron spin coupling constants, explains

the Curie temperature behavior of Cys50, is only valid if different coupling constants between the iron electronic spin and the nuclear $\beta\text{-CH}_2$ spin, A , are introduced. This becomes evident as the slope of the temperature dependence curves are maintained for both FdII_{ox} and FdII_{int} , as can be seen in Fig. 4. In order to reach a conclusion about the spin coupling alterations in FdII_{int} the A values need to be determined experimentally.

The empirical relationship between the chemical shifts of the hyperfine shifted $\beta\text{-CH}_2$ proton resonances and the $\text{Fe-S-C}\beta\text{-C}\alpha$ dihedral angles (θ), $\delta = a \sin^2 \theta + b \cos \theta = c$, is a modified Karplus equation that takes into account both π and σ mechanisms of spin delocalization [32]. The equation has been applied to the $[\text{3Fe-4S}]$ cluster containing proteins, *D. gigas* FdII and *Azotobacter vinelandii*, for which both NMR data and X-ray structures are available [18,33]. In this way it was possible to show that the angles vary on going from FdII_{ox} to FdII_{int} indicating that the environment at the cluster changes on breakage of the disulfide bond.

Direct evidence for the cleavage of the disulfide bridge has been obtained by inspection of the 2D-NOESY spectra of *D. gigas* FdII_{int} , and *D. gigas* FdII_{red} in the region where correlations between H_α of Cys18 and H_β of Cys42 are seen. The $\text{H}_\alpha\text{-H}_\beta$ cross peaks are seen to diminish when FdII_{ox} is reduced [31].

4. Conclusions

NMR has proved to be an unique tool to study small iron–sulfur containing proteins. Different redox states can be detected via NMR, structural changes in the cluster vicinity and electronic properties of the center can be investigated, and solution structures, even in the presence of a paramagnetic cluster, can be determined [13].

D. gigas FdII, being able to transfer three electrons in a single redox step, involving the $[\text{3Fe-4S}]$ cluster and taking the advantage of the presence of a disulfide bridge, is a fascinating electron transfer system. A further two electron reduction of the cluster, at redox potentials around -600 mV, leads to a formal $[\text{3Fe-4S}]^{2-}$ oxidation state. This state has been detected by electrochemical studies for several 7Fe containing proteins [34–36], and also for the 3Fe interconverted form of *Pyrococcus furiosus* (*P. furiosus*) Fd [37] and *D. gigas* FdII [38]. This implies that FdII can transfer a total of five electrons over a wide range of redox potentials.

Acknowledgements

Work supported by PRAXIS (JJGM) and JNICT (PBICT/BIO/95-ALM). We would like to thank Drs Victor Wray, Vincent Huynh, Eckard Münck, José Moura and Isabel Moura for their invaluable contribution and interest in this work.

References

- [1] R.H. Holm, in: R. Cammack, R.G. Sykes (Eds.), *Advances in Inorganic Chemistry*, vol. 38, Academic Press, 1992, pp. 1–71.
- [2] R.H. Holm, in: R. Cammack, R.G. Sykes (Eds.), *Advances in Inorganic Chemistry*, vol. 38, Academic Press, New York/London/Orlando, FL, 1992, pp. 281–322.
- [3] J.J.G. Moura, A.L. Macedo, P.N. Palma, in: H.D. Peck, J. LeGall (Eds.), *Methods in Enzymology*, vol. 243, Academic Press, New York/London/Orlando, FL, 1994, chap. 12.
- [4] H. Beinert, R.H. Holm, E. Münck, *Science* 277 (1997) 653.
- [5] J.J.G. Moura, I. Moura, T.A. Kent, J.D. Lipscomb, B.H. Huynh, J. LeGall, A.V. Xavier, E. Münck, *J. Biol. Chem.* 257 (1982) 6259.
- [6] T.A. Kent, J.L. Dreyer, M.C. Kennedy, B.H. Huynh, M.H. Emptage, H. Beinert, E. Münck, *Proc. Natl. Acad. Sci. USA* 79 (1982) 96.
- [7] S.J. George, F.A. Armstrong, E.C. Hatchikian, A.J. Thomson, *Biochem. J.* 264 (1989) 275.
- [8] T.A. Kent, B.H. Huynh, E. Münck, *Proc. Natl. Acad. Sci. USA* 77 (1980) 6574.
- [9] B.H. Huynh, J.J.G. Moura, I. Moura, T.A. Kent, J. LeGall, A.V. Xavier, E. Münck, *J. Biol. Chem.* 255 (1980) 3242.
- [10] A.J. Thomson, A.E. Robinson, M.K. Johnson, J.J.G. Moura, I. Moura, A.V. Xavier, J. LeGall, *Biochim. Biophys. Acta* 670 (1981) 93.
- [11] V. Papaefthymiou, J. Girerd, I. Moura, J.J.G. Moura, E. Münck, *J. Am. Chem. Soc.* 109 (1987) 4703.
- [12] S.A. Borshch, E.L. Bominaar, G. Blondin, J.J. Girerd, *J. Am. Chem. Soc.* 115 (1993) 5155.
- [13] B.J. Goodfellow, A.L. Macedo, *Annu. Rep. NMR Spectrosc.* 37 (1999) 119–177.
- [14] I. Bertini, C. Luchinat, *Coord. Chem. Rev.* 150 (1996) 29–75.
- [15] I. Bertini, C. Luchinat, *Coord. Chem. Rev.* 150 (1996) 77–110.
- [16] M. Bruschi, E.C. Hatchikian, J. LeGall, J.J.G. Moura, A.V. Xavier, *Biochim. Biophys. Acta* 449 (1976) 275.
- [17] M. Bruschi, *Biochim. Biophys. Res. Commun.* 91 (1979) 623.
- [18] C.R. Kissinger, L.C. Sieker, E.T. Adman, J.H. Jensen, *J. Mol. Biol.* 219 (1991) 693.
- [19] A.L. Macedo, I. Moura, K.K. Surerus, V. Papaefthymiou, M. Liu, J. LeGall, E. Münck, J.J.G. Moura, *J. Biol. Chem.* 269 (1994) 8052.
- [20] A.L. Macedo, I. Moura, J.J.G. Moura, J. LeGall, B.H. Huynh, *Inorg. Chem.* 32 (1993) 1101.
- [21] A.L. Macedo, P.N. Palma, I. Moura, J. LeGall, V. Wray, J.J.G. Moura, *Magn. Res. Chem.* 31 (1993) S59.
- [22] A.L. Macedo, J.J.G. Moura, in: G. LaMar (Ed.), *Nuclear Magnetic Resonance of Paramagnetic Macromolecules*, NATO-ARW, vol. 457, Kluwer Academic, Dordrecht, 1994, pp. 319–338.
- [23] B.H. Huynh, J.J.G. Moura, I. Moura, T.A. Kent, J. LeGall, A.V. Xavier, E. Münck, *J. Biol. Chem.* 255 (1980) 3242.
- [24] T.A. Kent, B.H. Huynh, E. Münck, *Proc. Natl. Acad. Sci. U.S.A.* 77 (1980) 6574.
- [25] L. Banci, I. Bertini, F. Briganti, *New J. Chem.* 15 (1991) 467.
- [26] L. Banci, I. Bertini, C. Luchinat, *Struct. Bonding* 72 (1990) 113.
- [27] S. Aono, I. Bertini, J.A. Cowan, C. Luchinat, A. Rosato, M.S. Viezzoli, *J. Biol. Inorg. Chem.* 1 (1996) 523.
- [28] I. Bertini, A. Dikiy, C. Luchinat, R. Macinai, M.S. Viezzoli, M. Vincenzini, *Biochemistry* 36 (1997) 3570.
- [29] B.J. Goodfellow, A.L. Macedo, I. Moura, V. Wray, J.J.G. Moura, *J.B.I.C.* (1998) in press.
- [30] J.G. Huber, J.M. Moulis, J. Gaillard, *Biochemistry* 35 (1996) 12705.
- [31] P. Rodrigues, A.L. Macedo, B.J. Goodfellow, I. Moura, J.J.G. Moura, *J. Biol. Chem.* (1998) submitted for publication.
- [32] I. Bertini, F. Capozzi, C. Luchinat, M. Piccioli, A.J. Vila, *J. Am. Chem. Soc.* 116 (1994) 651.
- [33] M.K. Trower, M.H. Emptage, F.S. Saislani, *Biochem. Biophys. Acta* 1037 (1990) 281.
- [34] J.N. Butt, F.A. Armstrong, J. Breton, S.J. George, A.J. Thomson, E.C. Hatchikian, *J. Am. Chem. Soc.* 113 (1991) 6663.

- [35] B. Shen, L.L. Martin, J.N. Butt, F.A. Armstrong, C.D. Stout, G.M. Jensen, P.J. Stephens, G.N. LaMar, C.M. Gorst, B.K. Burgess, *J. Biol. Chem.* 268 (1993) 25928.
- [36] J.L. Breton, J.L.C. Duff, J.N. Butt, F.A. Armstrong, S.J. George, Y. Pétillot, E. Forest, G. Schäfer, A.J. Thomson, *Eur. J. Biochem.* 233 (1995) 937.
- [37] E.T. Smith, J.M. Blamey, Z.H. Zhou, M.W.W. Adams, *Biochemistry* 34 (1995) 7161.
- [38] C. Moreno, A.L. Macedo, I. Moura, J. LeGall, J.J.G. Moura, *J. Inorg. Biochem.* 53 (1994) 219.